Detection of Tissue Inflammatory Change with Multifrequency 3-D Magnetic Resonance Elastography

Meng Yin[1], Kevin J. Glaser[1], Jun Chen[1], Yogesh K. Mariappan[1], Jayant A. Talwalkar[2], and Richard L. Ehman[1]
[1]*Radiology, Mayo Clinic, Rochester, Minnesota, United States,* [2]*Gastroenterology and Hepatology, Mayo Clinic, Rochester, Minnesota, United States*

Introduction: Multiple studies have reported on using hepatic MR Elastography (MRE) to quantitatively assess hepatic fibrosis by measuring the viscoelastic properties of the liver (1-3). In our harmonic hepatic MRE applications, "shear stiffness" (equal to tissue density – assumed to be 1 g/cm^3 – times the square of the shear velocity or wave speed) is usually assessed (2). Recent studies have shown that hepatic inflammation should be taken into account as a potential cause of variability of hepatic stiffness (4-5). The vascular reactions during inflammation are vasodilation and increased vessel permeability, which cause increased fluid volume and pressure (i.e., edema). It is likely that the use of additional mechanical properties other than "shear stiffness" will improve the identification of inflammatory changes of the liver. In some studies, complicated single or multifrequency material models are assumed to model tissue and the derivation of these model parameters can involve time-consuming inversion schemes and problematic translation to the diverse etiology of hepatic fibrosis (6-7). Thus, there is a need to consider if mechanical properties that can be derived immediately from a direct inversion of the equations of tissue motion (not assuming a specific poro- or viscoelastic model) are correlated with inflammation. The purpose of this study was to compare MRE-assessed mechanical properties from a hydrostatic porous phantom and a retrospective liver patient study to investigate which mechanical properties correlate with increased fluid pressure in phantoms and hepatic inflammation in humans.

Methods and Materials: *1) Phantom study:* When tofu is frozen, rupture stress increases due to physical compression caused by the growth of ice crystals (pore size) and the increase of chemical interactions caused by concentration changes during the freezing of proteins and salts (8). Once thawed, tofu will have a sponge-like texture. Degassed, frozen-then-thawed tofu submerged in different volumes of water was used as a biphasic model to simulate hepatic inflammation with varying (hydrostatic) fluid pressure and unchanged solid matrix viscoelasticity. Multifrequency (100, 120Hz) 3-D/3-axis MRE acquisitions were performed on the tofu phantom to obtain mechanical properties at two different hydrostatic pressures. As shown in the bottom left diagram of Fig. 1, the pressure difference between the two acquisitions was 68 mmH_2O (5 mmHg). The acquired 3-D/3-axis wave data had a resolution of 0.5x0.5x4 mm^3. The wave data were filtered with the curl operator to remove undesired bulk motion, processed with 20 evenly spaced 3-D directional filters (radial bandpass filter: 4th-order Butterworth filter, cut-off frequencies = (0.001, 40) cycles/FOV), smoothed with a 13x13x7 quartic kernel (9) and then inverted with a direct inversion (DI) of the Helmholtz equation. Mechanical properties reported included the complex shear modulus $G = G' + iG''$, the shear stiffness v_s^2, the attenuation α, and phase angle $\delta = \arctan(G''/G')$ at 100Hz and their differences between the two frequencies. *2) Retrospective patient study:* Our institution has performed over 100 multifrequency (40, 60Hz) 3-D/3-axis hepatic MRE exams on patients with chronic liver diseases. We reviewed 87 researchable exams in accordance with our Institutional Review Board. Liver biopsies were performed less than 1 year from the date of the MRE exam. Like in the phantom study, 3-D/3-axis wave data with 3x3x3 mm^3 resolution were filtered with the curl operator and 20 evenly spaced 3-D directional filters (cut-off frequencies = (0.001, 24) cycles/FOV), smoothed with a 5x5x5 quartic kernel, and then inverted to obtain the mechanical properties (v_s^2, α, G', G'', δ, and their dispersions). To obviate boundary issues, all quantities (reported as means and standard deviations over thousands of voxels) were collected in the central slices only. In the human study, contour profiles were used to investigate the interdependence of the mechanical properties and varying fibrosis/inflammation extent.

Results: As shown in the top half of Fig. 1, the tofu phantom had very good magnitude and phase SNR in the MRE images. Noticeable differences were found in several of the resulting mechanical property maps (e.g., v_s^2, G' and δ) when comparing results at the two pressures. Other than v_s^2 and G', there was no statistically significant difference in the other quantities (e.g., α and G'') due to the relatively large standard deviations of the measurements (as listed in the bottom right table of Fig. 1). The observed trends with increasing fluid pressure included 1) v_s^2 and G' increased; 2) α, G'' and δ decreased; and 3) no changes in the frequency dispersions of v_s^2, α, G', G'', and δ. Similar trends were found in the patient data analysis with coexisting inflammation (fluid pressure change) and fibrosis (solid matrix change) as shown in Fig. 2. Trends in the patient study included: 1) v_s^2 and its dispersion increased with fibrosis, and the vertical contours indicate that they are more sensitive to fibrosis stage than inflammation grade; 2) α and its dispersion decreased as inflammation and fibrosis stage increased; and 3) δ has similar behavior as the shear attenuation dispersion, with horizontal contours that indicate that they may be more sensitive to inflammation than fibrosis. Considering the standard deviations of all these quantities, v_s^2, G' and δ have smaller variances – compared with their means – than that of α and G''. Therefore, δ could be a potential indicator for fluid pressure or inflammation.

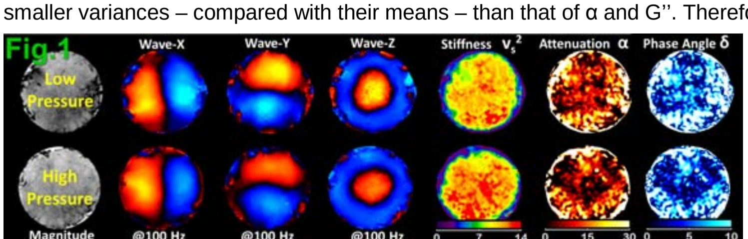

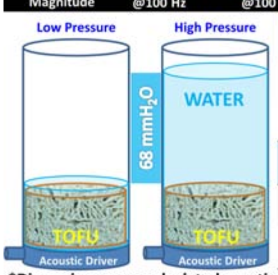

Model-free Properties	v_s^2 Shear Velocity^2	α Shear Attenuation	G' Storage Modulus	G'' Loss Modulus
Low Pressure	10.72 (0.86)	6.74 (5.47)	10.65 (0.85)	0.74 (0.61)
High Pressure	11.67 (0.87)	4.01 (6.46)	11.61 (0.89)	0.49 (0.78)
Model-free Properties	**δ Phase Angle**	**$\Delta v_s^2/\Delta f$ Dispersion***	**Δα/Δf Dispersion***	**Δδ/Δf Dispersion***
Low Pressure	4.51 (2.52)	0.16 (0.03)	0.31 (0.20)	0.17 (0.11)
High Pressure	3.68 (2.86)	0.15 (0.02)	0.30 (0.18)	0.17 (0.11)

*Dispersions were calculated as ratios of mechanical quantity changes between two frequencies.

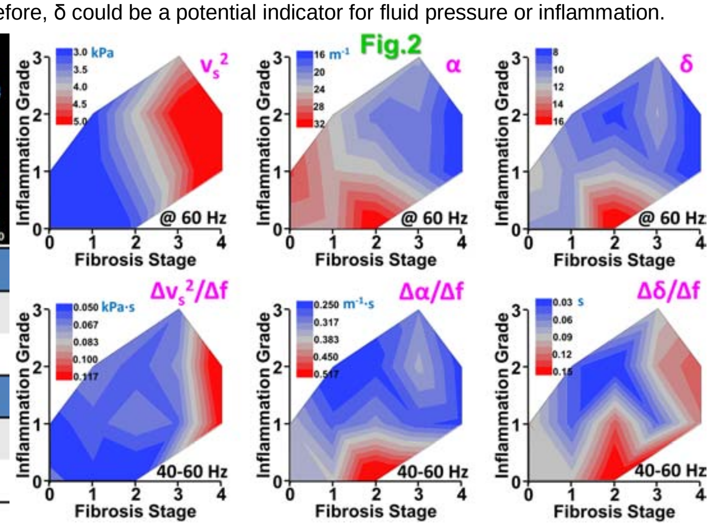

Discussion and Conclusion: Many groups have published findings on the mechanical properties of hepatic tissues, but the methods vary as widely as the values reported and their value in distinguishing inflammation and fibrosis remains a mystery. This preliminary study employed a simple yet robust inversion scheme to systematically investigate many possible mechanical properties for detecting fluid pressure change or hepatic inflammation. Though the utility of these quantities to assess inflammation remains to be established, our preliminary results on both phantom and patient data demonstrate that the shear modulus phase angle δ could be a potential indicator for differentiating inflammation. These findings offer preliminary evidence of the potential to extend MRE to distinguish and independently assess necroinflammatory and fibrotic processes.

References: 1. Huwart L, NMR Biomed 2006: 19(2):173-9; **2.** Yin M, Clin Gastroenterol Hepatol 2007: 5(10):1207-13; **3.** Klatt D, Phys Med Bio 2007: 52(24):7281-94; **4.** Chen J, Radiology 2011: 259(3):749-56; **5.** Salameh N, Radiology 2009: 253(1):90-7; **6.** Perrinez P.R., IEEE Trans Biom Eng 2009: 56(3):598-608; **7.** Doyley M. M., Phys. Med. Biol. 2012: 57:R35-R73; **8.** Fuchigami M. J.Food Sci.1998: 63(6):1054-57; **9.** Romano A, IEEE Trans Ultrason Ferroelectr Freq Control 2000: 47(6):1575-8.